Effective Hamiltonian for a microwave billiard with attached waveguide

H.-J. Stöckmann,[1] E. Persson,[2] Y.-H. Kim,[1] M. Barth,[1] U. Kuhl,[1] and I. Rotter[3]
[1]*Fachbereich Physik der Philipps-Universität Marburg, Renthof 5, D-35032 Marburg, Germany*
[2]*Institut für Theoretische Physik, Technische Universität Wien, A-1040 Wien, Austria*
[3]*Max-Planck-Institut für Physik Komplexer Systeme, D-01187 Dresden, Germany*
(Received 21 December 2001; published 25 June 2002)

In a recent work the resonance widths in a microwave billiard with attached waveguide were studied in dependence on the coupling strength [E. Persson *et al.*, Phys. Rev. Lett. **85**, 2478 (2000)], and resonance trapping was experimentally found. In the present paper an effective Hamiltonian is derived that depends exclusively on billiard and waveguide geometry. Its eigenvalues give the poles of the scattering matrix provided that the system and environment are defined adequately. Further, we present the results of resonance trapping measurements where, in addition to our previous work, the position of the slit aperture within the waveguide was varied. Numerical simulations with the derived Hamiltonian qualitatively reproduce the experimental data.

DOI: 10.1103/PhysRevE.65.066211 PACS number(s): 05.45.−a, 03.65.Nk, 84.40.Az

I. INTRODUCTION

In every measurement of the spectroscopic properties of a quantum mechanical system, the system must be coupled to an environment, unavoidably disturbing its properties. This is true even without performing a direct measurement, since most systems such as atomic nuclei are embedded in a continuum of decay channels due to which the states of the system have a finite lifetime. As a consequence, the measurement always yields a combination of the system properties and those of the environment.

An efficient tool to tackle this problem is provided by scattering theory (see [1]). The scattering matrix can be described by (see, e.g., Ref. [2], Chap. 6)

$$S=1-2\imath V^{\dagger}\frac{1}{E-H_{\mathrm{eff}}}V, \tag{1}$$

where

$$H_{\mathrm{eff}}=H-\imath VV^{\dagger}. \tag{2}$$

H is the Hamiltonian of the system with discrete eigenvalues e_α. V is the coupling matrix between the discrete states of the system and the channel wave functions of the environment.

Scattering theory was originally introduced in nuclear physics (see Ref. [3]). In recent years it has been applied to numerous other systems like quantum dots (e.g., [1]) and microwave cavities [4]. For spectra with high level density, statistical methods yield results such as the distributions of poles in the complex plane [5,6], the statistics of resonance poles, and delay times [7]. But for low level densities deviations have been observed and discussed [8–14]. These results suggest quantum mechanical interference effects between the quantum states. They are displayed, e.g., in the transport through quantum dots and microwave cavities, when the leads support only one or few propagating modes [15–18]. The interferences show clearly that at low level density the individual properties of the resonance states play an important role.

For *isolated* resonances the widths of the states are much smaller than the distances between them. Therefore the coupling matrix elements $V_{\alpha l}$ are well approximated by the overlap integrals between the wave functions ψ_α of the discrete states and the channel wave functions in the leads. The energies E_α are given by the eigenvalues e_α of the real part of H_{eff}, and the widths Γ_α are $\approx 2\Sigma_l(V_{\alpha l})^2$ [19]. This approximation is justified as long as the poles of the S matrix are close to the real axis [3]. These poles appear as isolated resonances of Breit-Wigner shape in the reaction cross section. This approach, which is the basis of random matrix theory, can be used also at low level density far from thresholds.

The situation changes considerably, however, when, as in many physical situations, the resonances *overlap* [8,19,20]. In such a case, the widths exceed the energetical distance between the resonances, thus causing a mixing of the resonance states via the continuum. Solving the eigenvalue equation

$$H_{\mathrm{eff}}\ \tilde{\phi}_\alpha=\tilde{\epsilon}_\alpha\tilde{\phi}_\alpha, \tag{3}$$

the pole representation of the scattering matrix reads [8,19]

$$S_{ll'}=S_{ll'}^{\mathrm{dir}}-2\imath\sum_\alpha\frac{\tilde{V}_{\alpha l}\tilde{V}_{\alpha l'}}{E-\tilde{\epsilon}_\alpha},\qquad \tilde{\epsilon}_\alpha=\tilde{E}_\alpha-\frac{\imath}{2}\tilde{\Gamma}_\alpha, \tag{4}$$

where $S_{ll'}^{\mathrm{dir}}$ describes the smooth part of the scattering matrix, and $\tilde{V}_{\alpha l}$ are the elements of the coupling matrix $\tilde{V}$ between the *resonance* states and the channel wave functions. A similar representation of the S matrix was considered in Ref. [21]. In general the $V_{\alpha l}$ depend on the energy of the system and the $\tilde{\phi}_\alpha$ are complex. Thus, the $\tilde{\epsilon}_\alpha$ and $\tilde{V}_{\alpha l}$ are energy dependent and complex as well. The eigenvalues of the effective Hamiltonian H_{eff} yield the poles of the S matrix lying at the solutions $E_\alpha=\tilde{E}_\alpha|_{E=E_\alpha}$, $\Gamma_\alpha=\tilde{\Gamma}_\alpha|_{E=E_\alpha}$ of the fixed-

point equations, when the system and environment are defined adequately. The $\tilde{V}_{\alpha l}$ have to be calculated by means of the eigenfunctions $\tilde{\phi}_\alpha$ of $H_{\rm eff}$ as discussed above; see Eq. (4). Indeed, the $\tilde{V}_{\alpha l}$ are complex and energy dependent in a nontrivial manner, as shown numerically for nuclei [22].

Dramatic changes were found in the wave functions of states with increasing resonance overlapping in a numerical study for the two-channel case in nuclear reactions [23]. As a result, two states of the system align with the channels and become short lived while the remaining ones decouple more or less strongly from the continuum of decay channels. This decoupling from the continuum is called *resonance trapping* [8]. Similar results have been found in calculations for molecules [24–26] and atoms [27–29]. In microwave cavities resonance trapping has been studied theoretically as a function of the opening of the cavity to an attached waveguide in the time delay function and in the mixing and biorthogonality of the eigenfunctions of the effective Hamiltonian and in its eigenvalues [30–32].

In many theoretical studies, the coupling matrix $VV^\dagger$ is assumed to be real and energy independent and the eigenvalues of the model Hamiltonian $H_{\rm eff}^{\rm mod}=H-\imath\beta VV^\dagger$ are studied as a function of increasing β. In such a case, the number of short-lived states is exactly equal to the number of open decay channels and the widths of the trapped states approach zero for large β values; see, e.g., [5,21,24]. In realistic systems, however, the parameter β cannot increase without limit [8,33–36]. Furthermore, the number of short-lived states may be much larger than the number of open channels, as has been shown in calculations for quantum billiards of Bunimovich type with different positions of the leads attached to the billiard [17].

Since there is much confusion in the literature about the concept of resonance trapping, let us first define in what way the term is used in this paper: Resonance trapping is a phenomenon appearing in open quantum systems. It is caused by the interaction of overlapping resonance states via the continuum of scattering states by which some of the states align with the channels by trapping other states. Therefore the total coupling strength is given by

$$\Gamma_t=\sum_{\alpha=1}^{N}\tilde{\Gamma}_\alpha\approx\sum_{\alpha=1}^{M}\tilde{\Gamma}_\alpha,\qquad\text{i.e.,}\qquad\sum_{\alpha=M+1}^{N}\tilde{\Gamma}_\alpha\approx 0,\quad(5)$$

where N is the number of states considered, and M is the number of short-lived states. Due to the reordering processes taking place in the system, the widths of the states are $\Gamma_\alpha=\tilde{\Gamma}_\alpha|_{E=E_\alpha}$. Resonance trapping occurs at fixed total coupling strength between the system and environment as a function of some parameter and can be observed if the total coupling strength is varied.

Hitherto there is only one experimental realization that has shown resonance trapping. It was found in a microwave billiard with attached waveguide, where the coupling strength could be controlled by means of a variable slit [37].

It is the purpose of this paper to show that the situation met in this experiment is indeed properly described by an effective Hamiltonian of type (2). In Sec. II we derive the effective Hamiltonian for the billiard with an attached waveguide and in Sec. III A the slit is included into the scattering theory. Numerical simulations and experimental results are presented in Secs. III B and III C. The results are summarized in the last section.

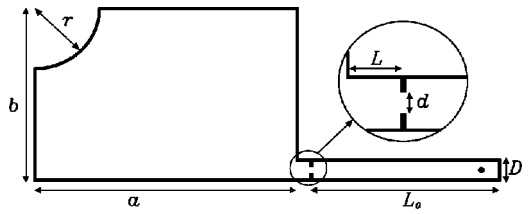

FIG. 1. Sketch of the billiard with attached waveguide and slit within the waveguide ($a=285$ mm, $b=200$ mm, $r=70$ mm, $L_0=204$ mm, $D=23.2$ mm, $L=5.5$ mm, 16 mm, and 26 mm).

II. WAVEGUIDE WITHOUT SLIT

Let us consider the situation of a billiard coupled by a waveguide to an environment. There are two limiting cases for the propagation of the channel modes inside the cavity.

(i) Waveguide and billiard have the same width. In this case the wave can propagate freely into the billiard. There are only small corrections from the evanescent modes in the threshold region [38].

(ii) The width of the waveguide is much smaller than the width of the cavity. In this case the wave can propagate only at the energies of the resonance states. Now the widths Γ_α of the states α are small and the S matrix poles are well described by Eq. (1).

In this paper we investigate the case where the lead extension is much smaller than the billiard width and a slit is introduced into the lead that can be closed.

Figure 1 shows the setup used in the experiment. We start with the case that there is no slit within the waveguide. One can show that the scattering matrix S of the billiard is given by (see Appendix A)

$$S=1-2\imath W^\dagger\frac{1}{E-H_{\rm eff}}WK,\quad(6)$$

where

$$H_{\rm eff}=H-\imath WKW^\dagger.\quad(7)$$

W is the coupling matrix between the billiard and waveguide eigenfunctions [see Eq. (A16)] and K is a diagonal matrix with the wave numbers $k_n=\sqrt{k^2-(n\pi/D)^2}$ for the waveguide modes on the diagonal, where D is the width of the waveguide. In the experiment only the lowest mode is propagating, and all others are evanescent, i.e., $k_n=\imath\lambda_n$ for $n\geqslant 2$ [Eq. (A12)]. We thus have a mapping of the billiard with attached waveguide to a scattering problem with an effective Hamiltonian. In the basis of billiard eigenfunctions the matrix elements of $H_{\rm eff}$ read

$$(H_{\rm eff})_{\alpha\beta}=E_\alpha\delta_{\alpha\beta}-\imath k_1W_{\alpha1}W_{\beta1}+\sum_{n=2}^{\infty}\lambda_nW_{\alpha n}W_{\beta n}.\quad(8)$$

The last term, $\Sigma_{n=2}^{\infty}\lambda_n W_{\alpha n}W_{\beta n}$, describes the influence of evanescent modes. It is nonvanishing only close to a threshold, as was shown in Refs. [38,39] where a very similar approach was applied.

It remains to rewrite Eq. (6) as a sum of pole terms according to the original definition of the S matrix, Eq. (4), by which the physical meaning of the S matrix poles is expressed. In order to stress the differences from the Hamiltonian approach to scattering used in the literature (e.g., Ref. [33]), we call this representation *pole representation* of the S matrix.

The diagonal coupling matrix element $\imath k_1 W_{\alpha 1}W_{\alpha 1}$ of $H_{\rm eff}$ induces an uncertainty in the energy of the state α due to which it becomes a resonance state with a certain width. As long as the resonance states are isolated, the resonances are of Breit-Wigner type with maximum at E_α and width $\Gamma_\alpha = 2k_1 W_{\alpha 1}W_{\alpha 1}$. In this regime, the Hamiltonian $H_{\rm eff}$ is almost diagonal and the pole representation of the S matrix (6) can be well approximated by

$$S = 1 - 2\imath \sum_\alpha \frac{k_1 W_{\alpha 1}W_{\alpha 1}}{E - E_\alpha + (\imath/2)\Gamma_\alpha}. \tag{9}$$

Numerically it has been shown that Eq. (9) is valid as long as the poles are in the near neighborhood of the real axis [33,40].

As soon as the resonance states are overlapping, a redistribution in the spectroscopic properties of the system takes place due to the nondiagonal terms $\imath k_1 W_{\alpha 1}W_{\beta 1}$ of $H_{\rm eff}$. The Hamiltonian $H_{\rm eff}$ has to be diagonalized,

$$H_{\rm eff}\tilde{\phi}_\alpha = [\tilde{E}_\alpha - (\imath/2)\tilde{\Gamma}_\alpha]\tilde{\phi}_\alpha. \tag{10}$$

The pole representation of the S matrix now reads

$$S = 1 - 2\imath \sum_\alpha \frac{k_1 \tilde{W}_{\alpha 1}\tilde{W}_{\alpha 1}}{E - \tilde{E}_\alpha + (\imath/2)\tilde{\Gamma}_\alpha} \tag{11}$$

where $\tilde{W}_{\alpha 1} = \langle W_1 | \tilde{\phi}_\alpha \rangle$, and W_1 is the first column of W. $\tilde{W}_{\alpha 1}$, $\tilde{E}_\alpha$, and $\tilde{\Gamma}_\alpha$ depend on the energy of the system and $\tilde{W}_{\alpha 1}$ are complex. The poles of the S matrix are obtained from the solutions of the fixed-point equations

$$E_\alpha = \tilde{E}_\alpha|_{E=E_\alpha} \qquad \text{and} \qquad \Gamma_\alpha = \tilde{\Gamma}_\alpha|_{E=E_\alpha}. \tag{12}$$

They determine the energies E_α and widths Γ_α of the resonance states. The eigenfunctions $\tilde{\phi}_\alpha$ of $H_{\rm eff}$ are biorthogonal. The resonances are no longer of Breit-Wigner type because of the energy dependencies of $\tilde{W}_{\alpha 1}$ and $\tilde{\Gamma}_\alpha$ (see [8,20]).

Therefore the reflection probabilities at the energies $\tilde{E}_\alpha$ of the resonance states are determined by the *complex energy-dependent* values $\tilde{W}_{\alpha 1}$ and not by the real energy-independent coupling matrix elements $W_{\alpha 1}$. The energy dependence of $\tilde{W}_{\alpha 1}$ ensures the unitarity of the S matrix (11). The total coupling strength

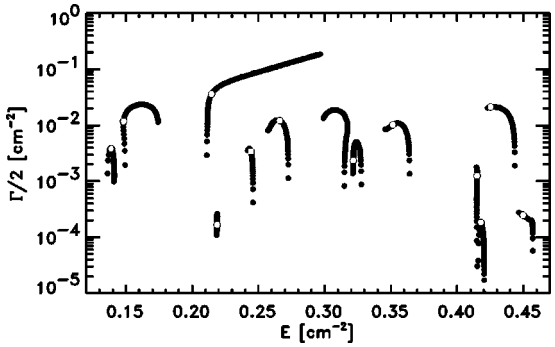

FIG. 2. The trajectories of the eigenvalues $\tilde{E}_\alpha(k) - (\imath/2)\tilde{\Gamma}_\alpha(k)$ of the effective Hamiltonian for different states α obtained by varying the energy. The open circles denote the solutions of the fixed-point equations. The geometry is that of Fig. 1 with $d = D = 91.6$ mm.

$$\Gamma_t = k_1 \sum_\alpha \tilde{W}_{\alpha 1}\tilde{W}_{\alpha 1} = k_1 \sum_\alpha W_{\alpha 1}W_{\alpha 1} \tag{13}$$

describes the coupling of the cavity to channel 1 at the energy E.

In Fig. 2, we show the trajectories of the eigenvalues of the Hamiltonian for a simulation with $D = 91.6$ mm (at maximum opening $d = D$). The solutions of the fixed-point equations (12) are marked on the eigenvalue trajectories. As E increases, first all $\tilde{\Gamma}_\alpha(k)$ increase, while at larger E most $\tilde{\Gamma}_\alpha(k)$ decrease with increasing E and only the $\tilde{\Gamma}_\alpha(k)$ of one of the resonance states increases further with E. The results show resonance trapping when the energy E of the system is parametrically varied. Moreover, they show clearly that the resonances are not of Breit-Wigner shape [corresponding to $\tilde{E}_\alpha(k) \approx$ const, $\tilde{\Gamma}_\alpha(k) \approx$ const]. In many cases, the energy dependence is quite strong. It is caused by the unitarity of the S matrix leading to a narrowing of most resonances at full opening of the cavity.

III. WAVEGUIDE WITH SLIT

A. Theory

In Eq. (6) the billiard scattering matrix was expressed in terms of an effective Hamiltonian for the case that the waveguide is coupled directly to the billiard. Now we proceed to the situation met in the experiment that a slit aperture with variable opening is placed within the waveguide (see Fig. 1).

The scattering matrix S is now given by

$$S' = \hat{g} + g e^{\imath KL}\frac{1+A}{2}e^{\imath KL}g - 2\imath g e^{\imath KL}\frac{1+A}{2}GK(1 + \imath AGK)^{-1}\frac{1+A}{2}e^{\imath KL}g, \tag{14}$$

where

$$A = 1 + (e^{-\imath KL} - \hat{g}e^{\imath KL})^{-1} 2\hat{g}e^{\imath KL} \tag{15}$$

(see Appendix B). The matrices g and $\hat{g}=1-g$ depend on the opening of the slit [see Eq. (B8)]; with increasing slit width g increases from 0 to 1.

Proceeding in the same way as before, we end up with

$$S' = \hat{g} + g e^{\imath KL} \frac{1+A}{2} e^{\imath KL} g - 2\imath g e^{\imath KL} \frac{1+A}{2} W^{\dagger} \frac{1}{E - H_{\text{eff}}} W K \frac{1+A}{2} e^{\imath KL} g, \quad (16)$$

where the effective Hamiltonian now is given by

$$H_{\text{eff}} = H - \imath W K A W^{\dagger}. \quad (17)$$

In expression (17), the properties of the billiard and the slit enter at different places. The eigenvalues and eigenfunctions of the billiard have therefore to be calculated only once. To study the eigenvalues of H_{eff} in dependence on the width and position of the slit, only A has to be recalculated. The coupling vector between the system and lead with the slit at the position L is, according to Eq. (17), $V^{\text{sl}}=\sqrt{KA}W$, while it is $V=\sqrt{K}W$ in the case without a slit [see Eq. (7)].

The position of the slit inside the lead introduces some arbitrariness in the separation of the complete function space into the subspace of the functions of the billiard and the supplementary subspace of the functions of the environment. The part of the lead between the slit and the billiard may belong to both subspaces: in the case of full opening it is part of the channel while it is part of the cavity if the slit is closed. In order to keep the physical meaning of the eigenvalues of H_{eff} and to relate them to the poles of the S matrix, we have to consider the value A in detail, to define the system and environment uniquely. Since only the first mode is propagating, only the behavior of the component A_{11} is of relevance in the present context.

According to Eq. (15), A_{11} has poles at the complex values $k_n=k_n^r+k_i^r=m\pi/L+i\ \ln(\hat{g}_{11})/2L$ (m integer). The case $L=0$ will not be discussed here in detail because experimentally it cannot be realized and theoretically some problems with the boundary conditions appear. For $L\neq 0$, the condition $k_n^r=m\pi/L$ describes a standing wave within the waveguide with momentum k_n^r appearing as an additional pole of the S matrix. It may be looked upon as an additional state of H_{eff} mixing with the other resonance states. The imaginary part of the momentum may be related to the width of the state. For $g\rightarrow 0$, corresponding to closing the slit, the imaginary part k_1^i vanishes and the state becomes discrete.

When the slit opens totally, i.e., $g\rightarrow 1$, from Eq. (15) it follows that $A\rightarrow 1$, and the imaginary part of k_1 diverges. The extra peak in A_{11}, arising from the resonance state localized in the waveguide between the billiard and the slit at $g=0$, thus disappears and the state is immersed in the subspace of channel wave functions representing the environment of the system. Thus, not only the subspace by which the system is defined (the first term H of H_{eff}) changes in varying g from 0 to 1; the subspace of channel wave functions into which the system is embedded at $g=1$ (open cavity) is also different from that at $g=0$ (closed cavity). When the slit is opened, the coupling vectors V are changing from $\sqrt{KA}W$, showing a resonant behavior as a function of energy, to $\sqrt{K}W$, while is smoothly dependent on energy. In other words, the relation between the direct and resonant processes changes on varying g. In the case of a fully open slit ($g=1,A=1$), the widths $\tilde{\Gamma}_R^c$ of all the cavity states are independent of the position of the slit.

The eigenvalues of H_{eff} have a physical meaning only when the total function space is divided into the two subspaces (system and environment) according to the following criteria: the system contains *all* resonancelike phenomena while the environment describes the smooth (direct) reaction part in the energy region considered. This division was used successfully by means of statistical methods for heavy nuclei about 50 years ago [41,42]. In light nuclei also division into the two subspaces is crucial for giving the eigenvalues of H_{eff} a physical meaning. This point is discussed in detail in Ref. [8]. Due to the low level density, the resonance states keep most of their individual features, and cannot be treated by statistical methods.

The numerical data for A, which will be discussed below, exhibit resonancelike features of $A(E)$ by which the division of the complete function space into the two subspaces is influenced. Since A is complex, the term $\text{Im}(WKAW^{\dagger})$ gives another contribution to $\text{Re}(H_{\text{eff}})$ which causes shifts of the resonances in the energy. In the following sections we present results of numerical simulations as well as of experimental studies which support the above discussion.

B. Numerical studies

For the numerics we use a width $D=22.9$ mm for the waveguide, which is close to the experimental value. Three different slit positions were taken at $L=5.5$, 16, and 26 mm, where L is the distance between cavity and slit. Only the first channel mode $n=1$ was considered, i.e., $1.88<E/\text{cm}^{-2}<7.52$.

In Fig. 3 we show the real part of k_1A_{11} [see Eq. (15)] for different g as a function of the energy E for the three different slit positions. First we note that with increasing slit width ($g\rightarrow 1$) the curves approach a single curve for all slit positions. For small g, however, the structure changes. The poles of A_{11} at $E_m=(m\pi/L)^2+(\pi/D)^2$ cause a resonancelike dependence as a function of E for $g<1$ (slit partly opened). This resonancelike behavior is an indication of the fact that the boundary between the subspaces of the discrete and scattering states changes. For full opening of the slit ($g=1$), A_{11} approaches 1, and the standing wave (the additional pole of the S matrix) vanishes and becomes part of the environment of the system consisting of the scattering wave functions. An analogous situation is discussed in detail for nuclei in Ref. [8]. As a result, the fixed-point solutions follow trajectories in energy space with increasing opening d that are different for the different positions L of the slit.

In the case of $L=5.5$ mm [Fig. 3(a)], the resonancelike behavior takes place at $E\gg 7\ \text{cm}^{-2}$. Therefore A increases monotonically with increasing opening of the slit (corresponding to increasing g) for almost all E. As a consequence, the components of the coupling vectors $V^{\text{sl}}=\sqrt{KA}W$ also

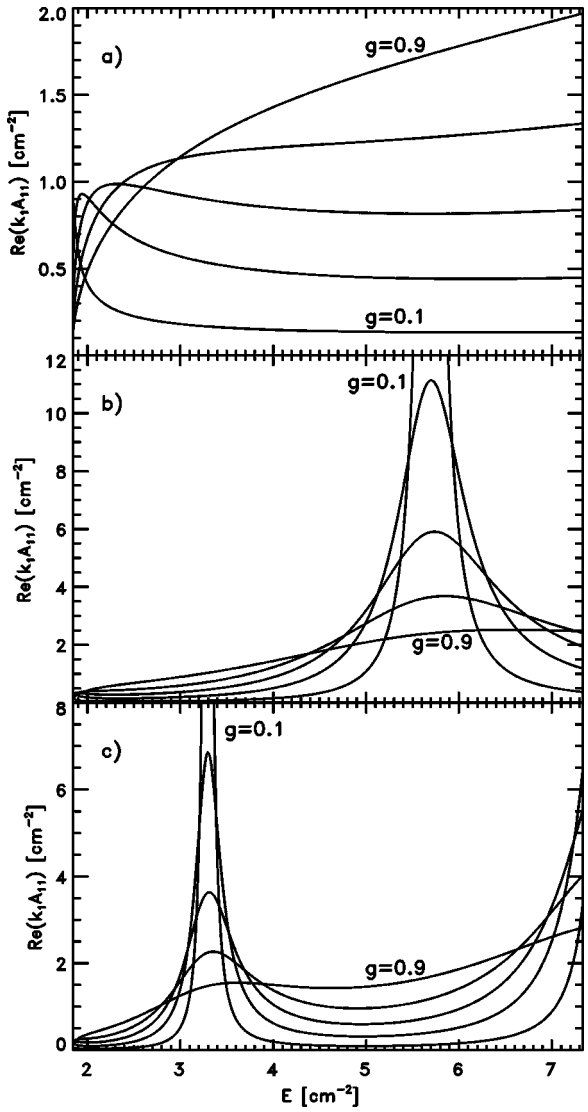

FIG. 3. $\mathrm{Re}(k_1 A_{11})$ defined by Eq. (15) for different g (0.1,0.3,0.5,0.7,0.9) as a function of the energy E for $L=5.5$ mm (a), 16 mm (b), and 26 mm (c). The width of the channel is $D=22.9$ mm.

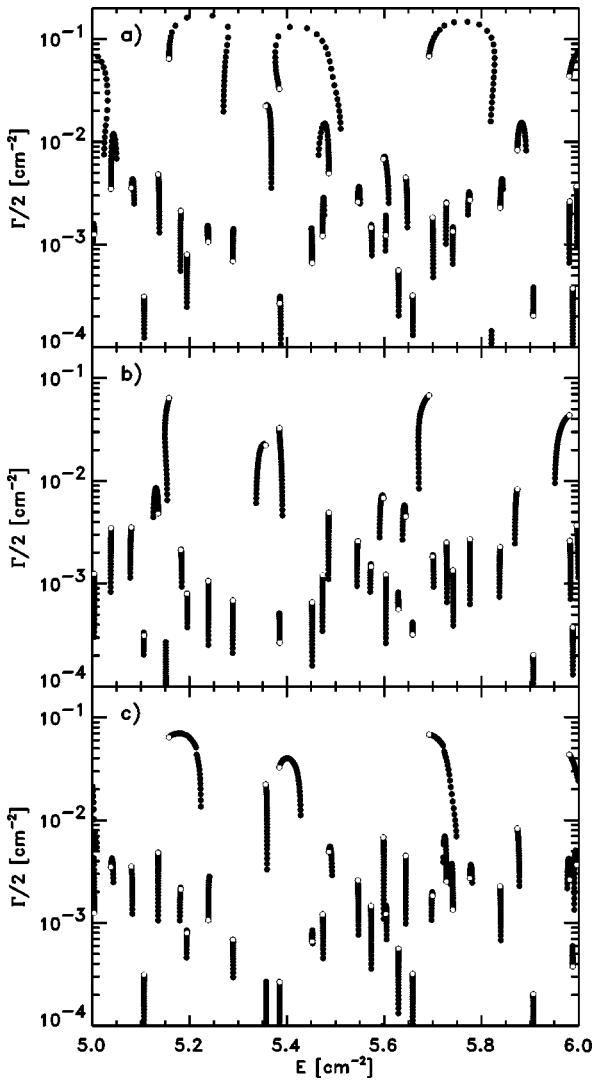

FIG. 4. The calculated eigenvalues for $L=5.5$ mm (a), 16 mm (b), and 26 mm (c). The open circles denote the eigenvalues at full opening ($d=D$).

increase monotonically with increasing opening for practically all E. We therefore expect resonance trapping in approaching the full opening.

In the case of $L=16$ mm, the first resonancelike behavior is within the energy region of interest. At the resonance A_{11} decreases strongly with increasing opening of the slit ($5<E/\mathrm{cm}^{-2}<6.6$). The width of the resonance of $A(E)$ increases with increasing opening [Fig. 3(b)]. It is difficult to decide whether this behavior of A will increase or reduce the probability of observing resonance trapping. Numerical studies have to be performed for the motion of the fixed-point solutions.

In the case of $L=26$ mm [Fig. 3(c)], the first resonancelike behavior becomes narrower and the second is approaching. In between there is a broad minimum. Due to the broad minimum and the narrow maximum we expect a similar situation to that for $L=5.5$ mm, at least in the range $4<E/\mathrm{cm}^{-2}<6.2$.

In Fig. 4, the motion of the fixed-point solutions E_α and Γ_α in the energy region $5.0\ \mathrm{cm}^{-2}\leqslant E_\alpha \leqslant 6.0\ \mathrm{cm}^{-2}$ is plotted in dependence on the slit width d for the three different positions of the slit ($L=5.5$, 16, and 26 mm). For small openings d, the widths of all N states increase with increasing d for all values of L. If d is further increased, however, different behavior is observed for the three cases considered. At $L=5.5$ and 26 mm resonance trapping can clearly be seen in the resonances. At $L=16$ mm, on the other hand, there are only a few cases of resonance trapping. Obviously, the existence of the pole in A decreases the probability for trapping. At full opening of the slit ($A=1$), the E_α and Γ_α of all the resonance states are the same for all three positions L of the slit.

C. Experimental studies

A microwave reflection measurement was performed on the system shown in Fig. 1. The system can be considered as two dimensional, as long as the frequency $\nu<c/2h$

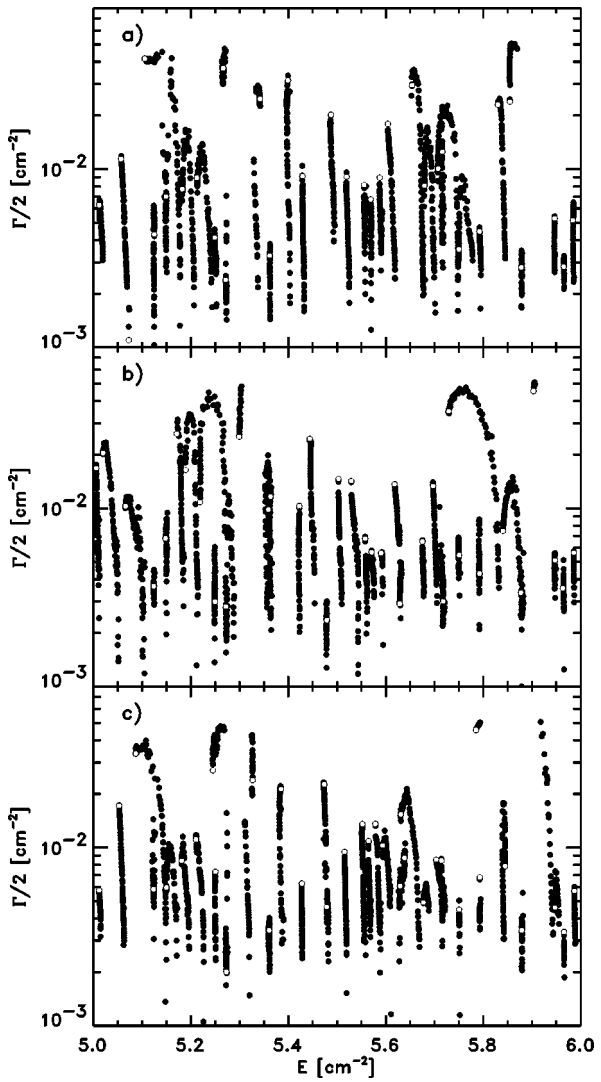

FIG. 5. The experimental eigenvalues, obtained by fitting the data to Lorentzians, for $L=5.5$ mm (a), 16 mm (b), and 26 mm (c). The open circles denote the eigenvalues at full opening ($d=D$).

$=18.75$ GHz (or $E/\mathrm{cm}^{-2}<15.4$), where $h=8$ mm is the resonator height. In this case there is a one-to-one correspondence between the wave function ψ and the electric field strength $\vec{E}_z$ (see, e.g., [2]).

In Fig. 5 experimental results for the three slit positions at $L=5.5$, 16, and 26 mm are shown. The resonances have been obtained by direct fitting of the complex reflection coefficients $R(k)$ by a superposition of Lorentzians. Using the centered time-delay analysis (CTDA) described in [37] similar results are obtained.

The differences in the trapping behavior are not as pronounced as in the case of the numerics and it is hard to see them in Fig. 5. This is due to some differences between the experiment and the simulation arising from the external part of the waveguide extending beyond the slit. In the experiment a small antenna induces the microwaves, and beyond that the waveguide is closed by a reflecting wall. This leads to additional interferences between the broad resonances (whose wave functions extend into the external waveguide) and the modes in the external waveguide. In the simulations, however, the external waveguide was assumed to be infinitely long, and no interferences between broad resonances and modes in the external waveguide could occur. Additionally, the resonances acquire an extra contribution to the widths due to the wall absorption that was not taken into account in the simulations.

TABLE I. The resonances (analyzed with CTDA) divided into three groups "trapped" (T), "broad" (B), and "others" (O). For details see text.

Length L (mm)	Numerics/ experiment	Number of resonances	T (%)	B (%)	O (%)	T/ B+O
5.5	N	90	50	19	31	0.98
	E	127	37	13	50	0.58
16	N	86	23	24	53	0.30
	E	107	26	8	66	0.35
26	N	86	44	17	39	0.79
	E	102	32	12	56	0.47

Due to these differences, we cannot expect a quantitative agreement between simulation and experiment. We will find, however, qualitative agreement for the influence of the length L on the degree of resonance trapping.

To show the qualitative agreement we divided the experimental and the numerical resonances into three groups according to their behavior as a function of the opening of the slit (Table I). The groups are defined as follows.

(1) Trapped: resonances decreasing in width at large openings.

(2) Broad: resonances gaining width at the cost of the trapped ones at some opening d of the slit. A resonance is classified as broad even if that resonance gets trapped by another resonance at larger d.

(3) All others.

The energy interval analyzed is $2.95\ \mathrm{cm}^{-2}\leqslant E\leqslant 6.85\ \mathrm{cm}^{-2}$. The experimental resonances could only be analyzed for $0.001\ \mathrm{cm}^{-2}\leqslant\Gamma_\alpha/2\leqslant 0.1\ \mathrm{cm}^{-2}$. We restricted the analysis of the numerical ones to the same width window. (Due to the wall absorption the experimental resonances have some extra width. Hence we analyzed more resonances in the experiment than in the numerics. This can be seen from the number of analyzed resonances in Table I.)

The division into the three groups is done on the basis of a careful tracing of all eigenvalue trajectories of the resonances as a function of d.

Most notably, both experiment and theory agree with respect to the L dependence of the trapping phenomenon: more resonances get trapped at $L=5.5$ and 26 mm than at $L=16$ mm in the experimental data as well as in the numerical ones as is evident from Table I.

Summarizing, we state the following: given the differences between the experiment and the assumptions for our theoretical study, the agreement between theory and experiment can be considered as good.

IV. SUMMARY AND CONCLUSIONS

An effective Hamiltonian H_{eff} has been derived for a billiard coupled to a waveguide with a slit, depending exclu-

sively on geometrical quantities. H_{eff} has complex eigenvalues, immediately giving the poles of the S matrix when the resonances do not overlap. The opening of the slit enters multiplicatively in the coupling matrix elements between billiard and waveguide. The eigenfunctions and eigenvalues of the billiard without waveguide have therefore to be calculated only once. For overlapping resonances, the two subspaces (system and environment) must be carefully defined before the energy-dependent eigenvalues of H_{eff} can be related to the poles of the S matrix by solving the fixed-point equations. The S matrix in pole representation is therefore different for the different positions of the slit inside the lead.

The theoretical formulas predict resonance trapping to occur more strongly at certain distances L between billiard and slit than at others. The numerical results show resonance trapping to depend on L as predicted, and the experiments on a microwave billiard agree qualitatively with the numerics results and theoretical predictions. The phenomenon of resonance trapping thus generically entails deviations from the randomness of the system properties.

ACKNOWLEDGMENTS

H. Schanz, Göttingen, is thanked for many useful remarks and discussions. The experiments were supported by the Deutsche Forschungsgemeinschaft. E.P. acknowledges support from FWF-SFB016.

APPENDIX A: *S* MATRIX OF A BILLIARD ATTACHED TO A WAVEGUIDE

If an infinitely long waveguide is coupled to a billiard (similar to the setup shown in Fig. 1), it is suitable to introduce a Green's function $G(r,r')$ with mixed boundary conditions. If r or r' is located on the billiard wall, one has $G(r,r')=0$, and $\nabla_\perp G(r,r')=0$ if they are located on the opening. $\nabla_\perp$ is the normal derivative pointing in the direction of the waveguide. The Green's function is defined by

$$G(r,r',E)=\left\langle r\left|\frac{1}{E-H}\right|r'\right\rangle=\sum_\alpha \frac{\psi_\alpha^*(r)\psi_\alpha(r')}{E-e_\alpha}, \tag{A1}$$

where H is the Hamiltonian, with discrete eigenvalues e_α and corresponding eigenfunctions $\psi_\alpha(r)$. It obeys the inhomogeneous Helmholtz equation

$$(\Delta+k^2)G(r,r')=\delta(r-r'). \tag{A2}$$

The wave function describing the field distribution within both the billiard and the channel obeys the homogeneous Helmholtz equation

$$(\Delta+k^2)\psi(r)=0 \tag{A3}$$

with the boundary condition $\psi(r)=0$ for r on the wall.

Multiplying Eq. (A2) by $\psi(r)$, Eq. (A3) by $G(r,r')$, taking the difference of the resulting equations, integrating over r, and applying Green's theorem, we obtain

$$\psi(r')=-\int_S G(r,r')\nabla_\perp\psi(r)\,dr, \tag{A4}$$

where the integration is over the width of the lead. All other contributions to the surface integral disappear due to the boundary conditions. Equation (A4) holds for the case that r' is a point within the billiard. For r' on the boundary there is an additional factor 1/2 on the right-hand side.

Applying a coordinate system with the positive x axis pointing along the waveguide and the y axis on the boundary, Eq. (A4) reads

$$\psi(0,y')=\frac{1}{2}\int_{-D/2}^{D/2} G(0,y;0,y')\frac{\partial\psi(0,y)}{\partial x}dy, \tag{A5}$$

where we have specialized Eq. (A4) to $x'=0$. Equation (A5) establishes a relation between the wave function and its normal derivative over the width of the lead. In the next step we expand the wave function within the lead in terms of channel eigenfunctions

$$\psi(x,y)=\sum_{n=1}^{\infty}\phi_n(y)(a_n e^{-\imath k_n x}-b_n e^{\imath k_n x}) \tag{A6}$$

where a_n and b_n are the amplitudes of the incoming and outgoing waves,

$$\phi_n(y)=\begin{cases}\sqrt{\dfrac{2}{D}}\cos\dfrac{n\pi}{D}y, & n \text{ even},\\ \sqrt{\dfrac{2}{D}}\sin\dfrac{n\pi}{D}y, & n \text{ odd},\end{cases} \tag{A7}$$

and

$$k_n=\sqrt{k^2-\left(\frac{n\pi}{D}\right)^2}. \tag{A8}$$

In the situation realized in our experiments only the first mode can propagate, and all others are evanescent, i.e., $k_n=\imath\lambda_n$, where

$$\lambda_n=\sqrt{\left(\frac{n\pi}{D}\right)^2-k^2} \quad \text{for} \quad n\geqslant 2. \tag{A9}$$

Putting the ansatz (A6) into Eq. (A5) we have

$$a_n-b_n=\imath\sum_m G_{nm}k_m(a_m+b_m), \tag{A10}$$

where

$$G_{nm}=\frac{1}{2}\int_{-D/2}^{D/2}dy\int_{-D/2}^{D/2}dy'\,\phi_n(y)\phi_m(y')G(0,y;0,y'). \tag{A11}$$

In matrix notation, Eq. (A10) reads

$$a-b=\imath GK(a+b), \tag{A12}$$

which follows

$$b = Sa, \tag{A13}$$

where

$$S = \frac{1 - \imath GK}{1 + \imath GK}. \tag{A14}$$

We have thus obtained the scattering matrix in terms of the billiard Green's function at the position of the lead.

Inserting expansion (A1) for the Green function into Eq. (A11) we get

$$G_{nm} = \sum_{\alpha} \frac{W_{\alpha n} W_{\alpha m}}{E - E_{\alpha}}, \tag{A15}$$

where

$$W_{\alpha n} = \sqrt{\frac{1}{2}} \int_{-D/2}^{D/2} \psi_{\alpha}(0,y)\, \phi_n(y)\, dy. \tag{A16}$$

Note that E_{α} and $\psi_{\alpha}(x,y)$ are eigenvalues and eigenfunctions of the billiard with mixed boundary conditions (Neumann at the boundary to the lead, and Dirichlet elsewhere). In short-hand notation Eq. (A15) reads

$$G = W^{\dagger} \frac{1}{E - H} W. \tag{A17}$$

Now we expand the denominator in Eq. (A14) into a geometric series and insert expression (A17) for G,

$$\begin{aligned} S &= 1 - 2\imath W^{\dagger} \frac{1}{E - H} WK \sum_{n=0}^{\infty} \left(-\imath W^{\dagger} \frac{1}{E - H} WK \right)^n \\ &= 1 - 2\imath W^{\dagger} \frac{1}{E - H} \sum_{n=0}^{\infty} \left(-\imath WKW^{\dagger} \frac{1}{E - H} W \right)^n WK. \end{aligned} \tag{A18}$$

Summing up again the geometric series we end up with the scattering matrix of Eq. (6).

APPENDIX B: *S* MATRIX WHEN A SLIT IS WITHIN THE WAVEGUIDE

First we calculate the transmission and reflection properties of the slit. Let

$$\psi_e(x,y) = \sum_n e_n \phi_n(y) e^{\imath k_n x} \tag{B1}$$

be a wave entering from the left, and

$$\psi_r(x,y) = -\sum_n r_n \phi_n(y) e^{-\imath k_n x} \tag{B2}$$

and

$$\psi_t(x,y) = \sum_n t_n \phi_n(y) e^{\imath k_n x} \tag{B3}$$

its reflected and transmitted fractions, respectively. Let us introduce the abbreviations

$$\int_{\mathrm{I}} dy = \int_{-d/2}^{d/2} dy, \qquad \int_{\mathrm{II}} dy = \left(\int_{-D/2}^{-d/2} + \int_{d/2}^{D/2} \right) dy. \tag{B4}$$

We then obtain for the reflection coefficients

$$r_n = \int_{\mathrm{II}} \psi_e(0,y)\, \phi_n(y)\, dy = \sum_m \hat{g}_{nm} e_m, \tag{B5}$$

where

$$\hat{g}_{nm} = \int_{\mathrm{II}} \phi_n(y)\, \phi_m(y)\, dy. \tag{B6}$$

Analogously we get for the transmission coefficients

$$t_n = \int_{\mathrm{I}} \psi_e(0,y)\, \phi_n(y)\, dy = \sum_m g_{nm} e_m, \tag{B7}$$

where

$$g_{nm} = \int_{\mathrm{I}} \phi_n(y)\, \phi_m(y)\, dy. \tag{B8}$$

By means of Eqs. (B5) and (B7) it is guaranteed that the field is zero on the walls of the slit, and continuous at the opening. From the orthogonality of the channel eigenfunction one has

$$g_{nm} + \hat{g}_{nm} = \delta_{nm}. \tag{B9}$$

Now let us assume that there is another wave $\psi'_e(x,y)$ entering from the right with reflected and transmitted fractions $\psi'_r(x,y)$ and $\psi'_t(x,y)$, respectively. The total field resulting from a superposition of all contributions is now given by

$$\psi(x,y) = \begin{cases} \displaystyle\sum_n \phi_n(y)[(-r_n + t'_n) e^{-\imath k_n x} + e_n e^{\imath k_n x}] & \text{(left)}, \\ \displaystyle\sum_n \phi_n(y)[e'_n e^{-\imath k_n x} + (t_n - r'_n) e^{\imath k_n x}] & \text{(right)}. \end{cases} \tag{B10}$$

Denoting as above the vector of amplitudes of the wave propagating to the left and to the right on the left-hand side by a,b, and on the right-hand side by a',b', and introducing corresponding vectors for reflection and transmission amplitudes, we have from Eq. (B10)

$$\begin{aligned} a &= t' - r, \qquad b = -e, \\ a' &= e', \qquad b' = r' - t. \end{aligned} \tag{B11}$$

Equations (B5) and (B7) and the corresponding relations for the primed quantities read in matrix notation

$$r=\hat{g}e, \qquad t=ge,$$
$$r'=\hat{g}e', \quad t'=ge'. \tag{B12}$$

Eliminating e,e',r,r',t,t' from Eqs. (B11) and (B12), we obtain

$$\begin{pmatrix} b' \\ a \end{pmatrix} = S_{\text{slit}} \begin{pmatrix} a' \\ b \end{pmatrix}, \tag{B13}$$

where

$$S_{\text{slit}} = \begin{pmatrix} \hat{g} & g \\ g & \hat{g} \end{pmatrix} \tag{B14}$$

is the scattering matrix for the slit. S_{slit} is unitary as it should be. This is a consequence of the projector properties of g and $\hat{g}$,

$$g^2=g, \qquad \hat{g}^2=\hat{g}, \qquad g\hat{g}=\hat{g}g=0, \tag{B15}$$

following immediately from the definitions (B6) and (B8).

Now we attach the waveguide to our previous billiard. Let us denote the scattering matrix of the billiard, including the waveguide up to the slit, by S_0, i.e.,

$$b=S_0 a. \tag{B16}$$

According to Eq. (A14) S_0 is given by

$$S_0 = e^{\imath KL}\frac{1-\imath GK}{1+\imath GK}e^{\imath KL}. \tag{B17}$$

The two additional phase factors $e^{\imath KL}$ account for the phase shifts acquired by the waves during propagation within the waveguide. Combining Eqs. (B13) and (B16) we obtain

$$b'=S'a', \tag{B18}$$

where

$$S'=\hat{g}+gS_0(1-\hat{g}S_0)^{-1}g \tag{B19}$$

is the scattering matrix for the complete system including billiard, waveguide, and slit. Inserting new expression (B17) for S_0 into Eq. (B19), we now end up with Eq. (14).

[1] T. Guhr, A. Müller-Groeling, and H.A. Weidenmüller, Phys. Rep. **299**, 189 (1998).

[2] H.-J. Stöckmann, *Quantum Chaos—An Introduction* (Cambridge University Press, Cambridge, England, 1999).

[3] C. Mahaux and H.A. Weidenmüller, *Shell-Model Approach to Nuclear Reactions* (North-Holland, Amsterdam, 1969).

[4] H. Alt *et al.*, Phys. Lett. B **366**, 7 (1996).

[5] F. Haake *et al.*, Z. Phys. B: Condens. Matter **88**, 359 (1992).

[6] N. Lehmann, D. Saher, V.V. Sokolov, and H.-J. Sommers, Nucl. Phys. A **582**, 223 (1995).

[7] Y.V. Fyodorov and H.-J. Sommers, J. Math. Phys. **38**, 1918 (1997).

[8] I. Rotter, Rep. Prog. Phys. **54**, 635 (1991).

[9] S. Tarucha *et al.*, Phys. Rev. Lett. **77**, 3613 (1996).

[10] R. Akis, D.K. Ferry, and J.P. Bird, Phys. Rev. B **54**, 17 705 (1996).

[11] J.P. Bird *et al.*, J. Phys.: Condens. Matter **9**, 5935 (1997).

[12] I.V. Zozoulenko, R. Schuster, K.-F. Berggren, and K. Ensslin, Phys. Rev. B **55**, R10 209 (1997).

[13] L. Wirtz, J.-Z. Tang, and J. Burgdörfer, Phys. Rev. B **56**, 7589 (1997).

[14] L. Wirtz, J.-Z. Tang, and J. Burgdörfer, Phys. Rev. B **59**, 2956 (1999).

[15] J.P. Bird *et al.*, Phys. Rev. Lett. **82**, 4691 (1999).

[16] Y.-H. Kim, M. Barth, H.-J. Stöckmann, and J.P. Bird, Phys. Rev. B **65**, 165317 (2002).

[17] R.G. Nazmitdinov, K.N. Pichugin, I. Rotter, and P. Šeba, Phys. Rev. E **64**, 056214 (2001).

[18] R.G. Nazmitdinov, K.N. Pichugin, I. Rotter, and P. Šeba, e-print cond-mat/0111301 (unpublished).

[19] The $V_{\alpha l}$ and $\tilde{V}_{\alpha l}$ stand for the partial width amplitudes of isolated and overlapping resonance states, respectively, as defined in nuclear physics. They differ by a factor $\sqrt{\pi}$ from the coupling matrix elements W_R^c and $\tilde{W}_R^c$ defined in [20] as well as from the coupling matrix elements used in the Hamiltonian approach to scattering; see, e.g., [33].

[20] I. Rotter, Phys. Rev. E **64**, 036213 (2001).

[21] V.V. Sokolov and V.G. Zelevinsky, Nucl. Phys. A **504**, 562 (1989).

[22] S. Drożdż, J. Okołowicz, M. Płoszaczak, and I. Rotter, Phys. Rev. C **62**, 024313 (2000).

[23] P. Kleinwächter and I. Rotter, Phys. Rev. C **32**, 1742 (1985).

[24] F. Remacle, M. Munster, V.B. Pavlov-Verevkin, and M. Desouter-Lecomte, Phys. Lett. A **145**, 365 (1990).

[25] M. Desouter-Lecomte and V. Jaques, J. Phys. B **28**, 3225 (1995).

[26] F. Remacle and R.D. Levine, Phys. Lett. A **211**, 284 (1996).

[27] V.V. Flambaum, A.A. Gribakina, and G.F. Gribakin, Phys. Rev. A **54**, 2066 (1996).

[28] A.I. Magunov, I. Rotter, and S.I. Strakhova, J. Phys. B **32**, 1669 (1999).

[29] A.I. Magunov, I. Rotter, and S.I. Strakhova, J. Phys. B **34**, 29 (2001).

[30] E. Persson, K. Pichugin, I. Rotter, and P. Šeba, Phys. Rev. E **58**, 8001 (1998).

[31] P. Šeba *et al.*, Phys. Rev. E **61**, 66 (2000).

[32] I. Rotter, E. Persson, K. Pichugin, and P. Šeba, Phys. Rev. E **62**, 450 (2000).

[33] K.N. Pichugin, H. Schanz, and P. Šeba, Phys. Rev. E **64**, 056227 (2001).

[34] U. Peskin, H. Reisler, and W.H. Miller, J. Chem. Phys. **101**, 9672 (1994).

[35] I. Rotter, J. Chem. Phys. **106**, 4810 (1997).

[36] U. Peskin, H. Reisler, and W.H. Miller, J. Chem. Phys. **106**,

4812 (1997).
[37] E. Persson, I. Rotter, H.-J. Stöckmann, and M. Barth, Phys. Rev. Lett. **85**, 2478 (2000).
[38] G.B. Akguc and L.E. Reichl, Phys. Rev. E **64**, 056221 (2001).
[39] L.E. Reichl and G. Akguc, Found. Phys. **31**, 243 (2001).
[40] S. Ree and L.E. Reichl, Phys. Rev. B **59**, 8163 (1999).
[41] H. Feshbach, Ann. Phys. (N.Y.) **5**, 357 (1958).
[42] H. Feshbach, Ann. Phys. (N.Y.) **19**, 287 (1962).